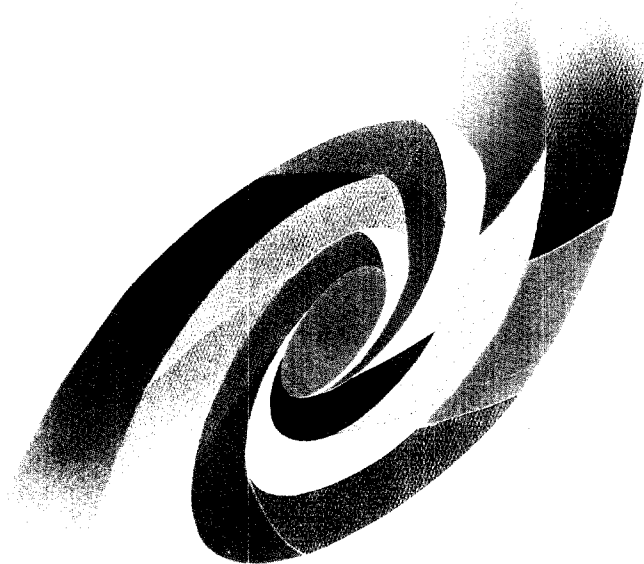$\varepsilon\varepsilon$

cea
C.E. SACLAY
DSM

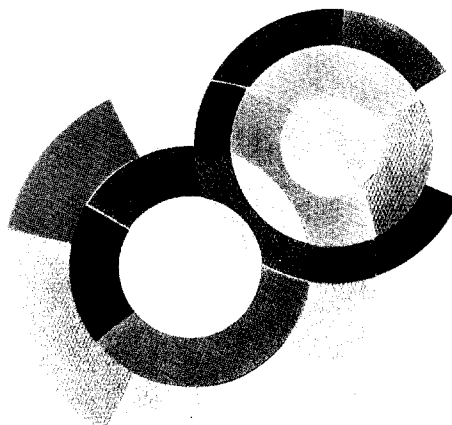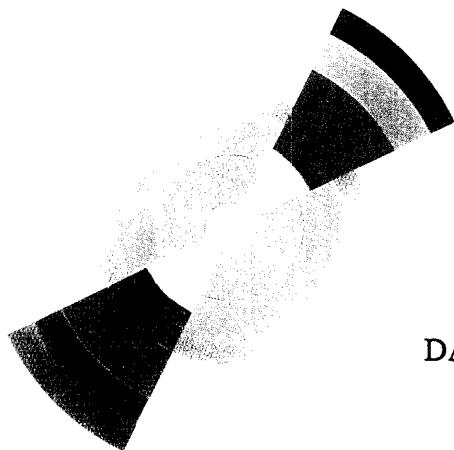# SERVICE D'ÉTUDE DES ACCÉLÉRATEURS

$S\sim 0807$

DAPNIA/SEA-97-16   11/1997

Future Lepton Colliders

A. Mosnier

DAPNIA

Le DAPNIA (**D**épartement d'**A**strophysique, de **p**hysique des **P**articules, de physique **N**ucléaire et de l'**I**nstrumentation **A**ssociée) regroupe les activités du Service d'Astrophysique (SAp), du Département de Physique des Particules Elémentaires (DPhPE) et du Département de Physique Nucléaire (DPhN).

Adresse :   DAPNIA, Bâtiment 141
                   CEA Saclay
                   F - 91191 Gif-sur-Yvette Cedex

Invited talk given at the XVIII Int. Symposium on Lepton and Photon Interactions, Hamburg, 28 July - 1 August 1997

FUTURE LEPTON COLLIDERS

A. MOSNIER

*Commissariat à l'Energie Atomique, Division des Sciences de la Matière,
CEA/Saclay, 91191 Gif-sur-Yvette Cedex, France*

Lepton colliders in the TeV range will extend and complement experiments done at the LHC, with unique opportunities for both discovery and precision measurement. Over the past ten years there has been a concerted effort to study physics goals and requirements, and in parallel to develop accelerator physics and technologies. The various schemes, which are all presently explored in different laboratories within a world-wide collaboration, are reviewed and discussed : those based on the very mature linear electron-positron collider, as well as the more recently revisited muon collider.

1 Lepton Colliders Overview

During the past decades, accelerator facilities with colliding beams have been playing a major role in exploring the elementary particle physics along the high energy frontier. Complementary to hadron colliders, either in operation or under construction - like the Large Hadron Collider (LHC) at CERN - the lepton colliders will provide unique opportunities for both discovery and precision measurement. As a matter of fact, lepton machines involve well-defined initial state and result in clean final states. They generate interactions between the fundamental constituents of the colliding beams and the full machine energy is available for physics. Electron colliders operate in two distinct energy ranges.

1.1 Low energy regime

In the lower energy regime, these facilities are generally tuned to the resonance of a heavy quark-antiquark bound state and are exclusively based on circular accelerators. The expected, or close to be achieved, luminosities of typical circular e^+e^- colliders are reproduced in Table 1. The highest luminosity presently attained is 4×10^{32} $cm^{-2}s^{-1}$ at the CESR facility and should rise beyond 10^{33} after some hardware improvements. Asymmetric colliders, like PEPII or KEKB, on the point of commissioning, aim at providing even higher luminosities. For higher energies, the ring concept fails because of the synchrotron radia-

Table 1: Luminosities of typical circular e^+e^- colliders

		LEP2	DAΦNE	CESR	PEPII	KEKB
E_{beam}	GeV	≈ 92	0.51	4.7-5.8	3.1 + 9	3.5 + 8
$\mathcal{L}$	$cm^{-2}s^{-1}$	$\leq 10^{32}$	$5\ 10^{32}$	10^{33}	$3\ 10^{33}$	10^{34}

tion, which scales as 4th power of the beam energy. A cost minimum is then obtained when the cost of the ring ($\propto$ radius ρ of the ring) is balanced by the cost of the RF needed to replace the synchrotron energy loss ($\propto E^4/\rho$), i.e. when both cost and size are proportional

to the energy squared. Therefore, circular e^+e^- colliders can reach very high luminosities thanks in particular to the high collision frequency, but are limited in energy by synchrotron radiation. The Large Electron Positron (LEP) at CERN, with a circumference of 27 km, has reached an economical limit (at $\approx 200\,$GeV c.m. energy) and will be probably the last high energy e^+e^- circular machine.

1.2 High energy regime

The only possibility to impart higher momenta to electrons is to build two linacs facing each other. However, the bunches can be used only once and must therefore have extremely small transverse dimensions in order to achieve the desired luminosity. Since fundamental cross sections fall as the square of the c.m. energy, the luminosity must rise as the square of the collider energy. The resulting target luminosity to keep a reasonable rate of events, is then the following

$$\mathcal{L} \approx 10^{34} \left(\frac{E_{c.m.}}{1\,TeV} \right)^2 cm^{-2} s^{-1}$$

Present Linear Colliders designs have an initial c.m. energy of about $500\,$GeV with luminosity in excess of $10^{33}\ cm^{-2} s^{-1}$ and are expandable to 1 TeV and beyond. But going to much higher energies will be difficult. In particular, increasing luminosity amounts to increasing electromagnetic fields at the collision point, thus intensifying beam-beam effects. Since beamstrahlung is a background source for the detector, it is a limiting factor for luminosity. Moreover, going to higher multi-TeV energies increases dramatically the coherent e^+e^- pairs from the beamstrahlung photons. If the beam-beam related backgrounds cannot be solved, other 'beamstrahlung-free' schemes have to be considered.

1.3 Beamstrahlung-free schemes

One possibility is charge compensation, but it seems difficult to realize. The beam fields could be neutralized either by co-moving beams with opposite charge or by plasma return-currents. In the former method, control of the overlapping electron and positron beams, as well as stability of the neutralization process are real problems. In the latter method, significant backgrounds from interactions in the plasma are expected.

A second approach is the $\gamma - \gamma$ collider. The photon beams are generated by Compton backscattering of intense laser beams (of a few μm wave-length) which are focused on the high energy electron beams just before the interaction point (IP). The critical issues are the development of high power lasers - which could be Free Electron Lasers - with adequate repetition rate, and the removal of the spent electron beams to avoid background. The $\gamma - \gamma$ collisions could be an option in any e^+e^- collider, because of the relatively small additional cost.

Lastly, muon colliders offer numerous advantages and would solve the beamstrahlung problem because massive particles are far less sensitive to the beam-beam effects. The challenges are however many and come mainly from the μ-decay, with a lifetime of about $2.2\,\mu$s at rest. Each of the components of the collider has significant technological or beam dynamics issues and needs intensive Research and Development.

2 Linear e^+e^- Colliders

Over the last ten years detailed design parameters have been developed and extensive accelerator physics and technological studies have been carried out for linear colliders. Various possible approaches have emerged within the framework of a world-wide collaboration and a series of workshops was held to address the main issues of such a collider. The efforts focused on high luminosity colliders - in excess of 10^{33} $cm^{-2}s^{-1}$ - with initial c.m. energy of 500 GeV, expandable to 1 TeV and beyond. With respect to the unique Linear Collider presently operational, the SLC at SLAC, the requested performance has to be improved by a factor ten in beam energy and by more than three orders of magnitude in luminosity. Fig.1 shows for example a luminosity history at the SLC[10]. The peak luminosity reached so far is 0.8×10^{30} $cm^{-2}s^{-1}$ with the added feature of 80% polarization of the electron beam. The collider, which has just attained the design luminosity, is a very useful tool for learning
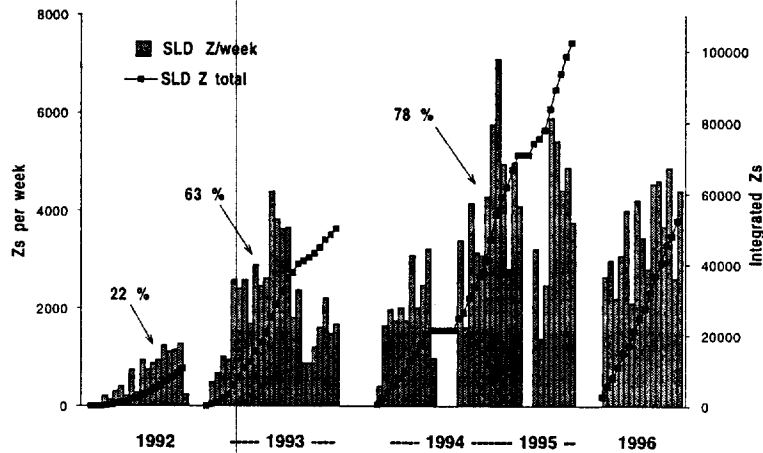

Figure 1: Luminosity history in the SLC.

about accelerator physics and operational issues relevant to a future linear collider

2.1 Luminosity and beam parameters

General constraints on the beam parameters arise from beam-beam effects at the IP. In terms of colliding beam parameters, the luminosity is given by the well-known expression:

$$\mathcal{L} = \frac{N^2 f_c}{4\pi\,\sigma_x\sigma_y} \qquad (1)$$

where f_c is the collision frequency, N the number of particles per bunch and the denominator is the beam spot area. A schematic view of the beam-beam phenomenon is sketched on Fig.2. Because of the strong electromagnetic fields, the bunches are fairly focused during the collision, leading to the pinch effect of one bunch by the other one. Besides, the particles emit intense synchrotron radiation due to the high magnetic field. The magnitude of the electromagnetic fields is generally parametrized by Υ, which can be estimated for beams with Gaussian charge distribution:
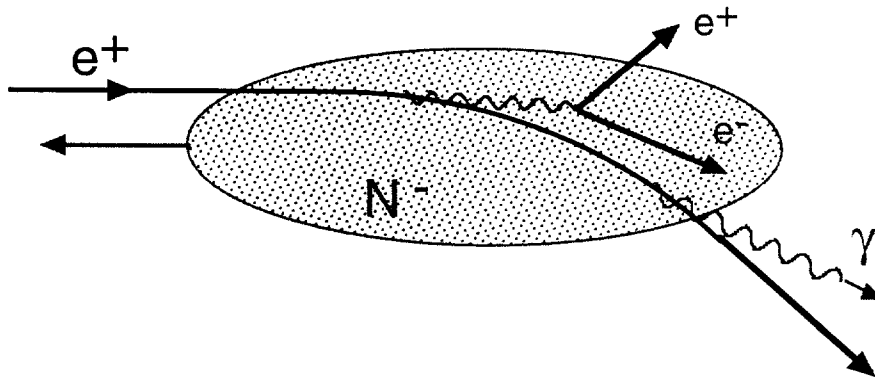
Figure 2: Schematic drawing of beam-beam effects.

$$\Upsilon = \gamma \frac{B}{B_c} = \frac{5r_e^2}{6\alpha} \frac{\gamma N}{\sigma_z(\sigma_{\mathrm{x}} + \sigma_{\mathrm{y}})} \tag{2}$$

with the classical electron radius r_e, the Lorentz factor γ, the fine structure constant α and the transverse and longitudinal rms beam sizes $\sigma_x, \sigma_y, \sigma_z$. Noting that this beamstrahlung parameter is proportional to the beam energy, we can distinguish roughly two energy regimes:

- For energies below 1 TeV, Υ is much lower than unity and the classical treatment of radiation effect can be applied.

- For energies above 1 TeV, Υ is larger than unity and the so-called quantum regime is achieved, because the critical radiation energy would exceed the incoming particle energy.

In the last regime, phenomena such as coherent pair production, where the beamstrahlung photons are converted in the strong field of the whole on coming bunch, could increase backgrounds dramatically. For all present designs Υ is slightly smaller than 0.3. Then the pairs are only produced by the incoherent interaction of photons on individual particles of the oncoming beam, but few of them will hit the detector.

The luminosity in Eq.1 can also be written as

$$\mathcal{L} = \frac{1}{4\pi E} \frac{P_{\mathrm{b}}}{\sigma_{\mathrm{y}}} \frac{\gamma N}{\sigma_x} \tag{3}$$

The second factor tells us to maximize the total beam power and to minimize the vertical spot size at the same time. It will address the main issues of the accelerator technology : high efficiency linacs to deliver high beam power without excessive wall plug power (around 100 MW), and tight tolerances, low beam emittances, strong final focus to achieve the required tiny spot sizes. The last factor determines the number of beamstrahlung photons emitted during the collision and is hence highly constrained by background levels in detectors.

4

Lastly, another useful expression for luminosity can be given in terms of the beam-strahlung energy loss δ_B, usually a few percents, which describes the smearing of the luminosity spectrum by the radiation during the beam-beam interaction:

$$\mathcal{L} = A \frac{P_b}{\gamma} \sqrt{\frac{\delta_B}{\varepsilon_y}} \qquad (4)$$

with $A \approx 10^{36} \mathrm{cm}^{-2}\mathrm{s}^{-1}$, ε_y the normalized vertical emittance and P_b in MW. This alternate expression assumes a vertical beam size much lower than the horizontal one, and the optimal focusing for the hour-glass effect. Again, as the beamstrahlung energy loss is constrained to a few percents, a large beam power and a small vertical emittance must be sought.

2.2 The different approaches

Although various linear colliders are presently studied, the overall layout is roughly the same for all designs. Fig.3 recalls the generic layout of such a collider: electron and positron
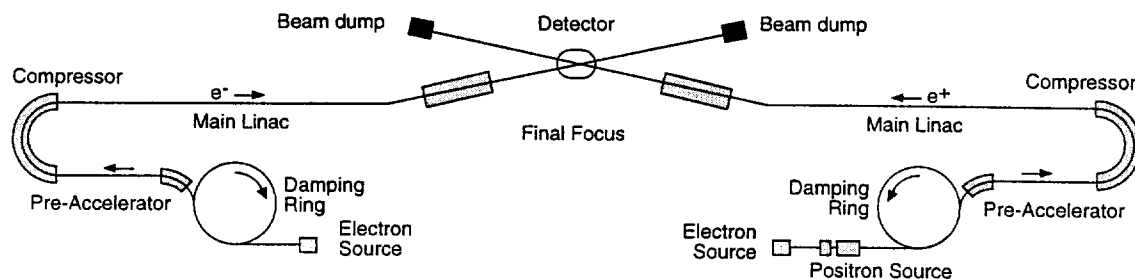

Figure 3: Generic layout of a linear collider.

sources produce the beams, damping rings shrink the beam emittances, compressors and pre-accelerators prepare the bunches for acceleration, main linacs accelerate the beams to high energy, final focus demagnifies the beam sizes for collision and detector must have clean environment and low backgrounds. The different designs differ mainly by the main linac acceleration scheme and the RF frequency covers a wide range from 1.3 GHz to 30 GHz. The concepts are summarized on Fig.4 in ascending order of frequency. From 3 GHz to 14 GHz, copper structures and pulsed klystrons are used. This approach rely on an extrapolation of conventional technology. It requires high RF peak power and generates strong wakefields. In the lower range, the TESLA scenario uses superconducting Niobium cavities. The main features are a low RF peak power, small wakefields and a high wall plug to beam power efficiency. The challenges lie in the accelerating gradient and the cost reduction of the linac. Lastly, in the higher frequency range, the two-beam concept can afford to achieve high gradients. Klystrons are replaced by a low energy drive beam running parallel to the main linac and tranfering periodically the RF power. The main difficulties consist in the drive beam generation and the very strong wakefields. The table at the bottom of Fig.4 indicates typical parameters of the colliders at 500 GeV c.m. energy. The gradients range from 17 to 95 MV/m, the vertical spot sizes from 3 to 19 nm and the highest beam power is proposed for the superconducting scheme.

5

TESLA	SBLC	JLC-C	JLC-X	NLC	VLEPP	CLIC
1.3 GHz	3 GHz	5.7 GHz	11.4 GHz	11.4 GHz	14 GHz	30 GHz

Superconducting Nb-cavities		Cu structures & klystrons				Two-Beam
low rf-peak power small wakefields high efficiency		conventional technology extrapolation				high gradients "no" klystrons
challenge of gradient & Qo cost reduction		high rf-peak power strong wakefields				drive beam generation very strong wakefields

Parameters at Ecm = 500 GeV (Luminosity ≈ 3-6 10^{33} cm^{-2}s^{-1})

		TESLA	SBLC	JLC-C	JLC-X	NLC	VLEPP	CLIC
G	(MV/m)	25	17	33	58	35	91	95
L_{tot}	(m)	32	35	22	14	28	10	10
σ_y^{IP}	(nm)	19	15	4	3	6	4	5
P_{beam}	(MW)	8	7	3	3.6	4.8	2.4	4.5

Figure 4: Overview of linear collider concepts.

2.3 Beam quality preservation

In order to achieve the desired luminosity, beams with very small emittances must be generated by the injector complex and then accelerated to the final energy through several km long linacs. Preservation of the beam quality during acceleration is then of main concern. The three primary sources of emittance dilution are the short and long range transverse wakefields, the dispersive and chromatic effects and the transverse jitter induced by quadrupole motion. Whereas the first source requires a strong focusing system, the last ones are intensified by a stronger focusing.

Short-range Wakefield effects

When the beam enters off-center into a structure, it excites transverse wakefields, which deflect the trailing particles. For short-range wakefields, the tail of a bunch is deflected by the head, whereas for long-range wakefields, bunches of a train are deflected by all previous bunches. As longitudinal and transverse wakefields scale approximately with the second and third power of the RF frequency, lower effects will be obtained with lower frequency linacs. When, for example, some errors in structure alignment are considered, transverse wakefields will produce differential kicks along the bunch and will therefore generate emittance growth. For illustration, Fig.5 shows the distortion of the bunch (large circles) as it proceeds down the linac. The dots are the particles in the transverse phase space, from which the emittance growth can be inferred. Having a glance at the expression Eq.5 of the emittance growth
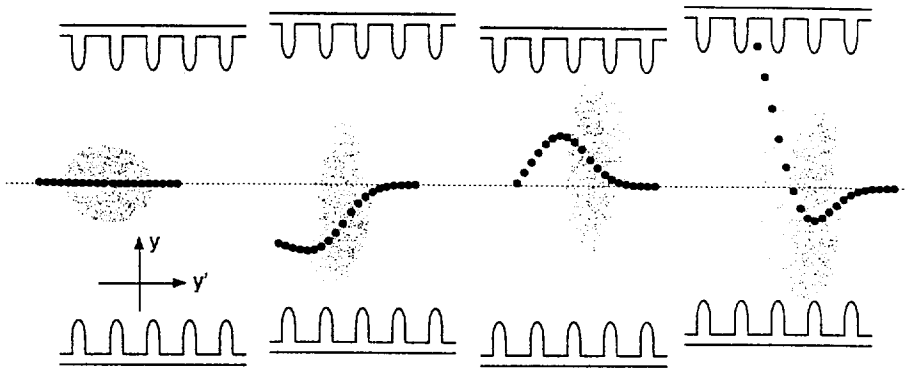
6

Figure 5: Bunch distortion due to accelerator misalignment.

induced by random structure offsets, we note a very strong frequency dependence. This ω_{rf} dependance must be compensated in high frequency designs by stronger focusing optics and more stringent alignment tolerances.

$$\frac{\Delta\varepsilon}{\varepsilon} \propto \frac{N^2\omega^6\sigma_z}{\varepsilon F(foc)}\frac{L_s}{G}d_{rms}^2 \qquad (5)$$

with the bunch population N, the bunch length σ_z, the structure length L_s, the gradient G, the alignment error d_{rms} and the function $F(foc)$ describing the focusing strength.

The order of magnitude of the tolerances (μm) on the accelerating structure positionning in the different designs is given in Table 2. After a cautious pre-alignment by conventional

Table 2: tolerances (μm) on the accelerating structure positionning

TESLA	SBLC	JLC	NLC	CLIC
500	30	10	10	2

methods, additional correction techniques are required to decrease the beam dilution in the designs demanding the most stringent tolerances. For example, the accelerating structures will be finely re-aligned with precision movers, by monitoring the dipole wakefield signals induced by the off-axis beam.

Long-range Wakefield effects

In order to reduce the beam-beam effects and also to improve the wall plug to beam power, all designs - except VLEPP - distribute the high beam charge at each RF pulse into multiple lower charge bunches. On the other hand the cumulative beam breakup, due to the long-range transverse wakefields, can cause harmful multibunch instabilities and must be carefully controlled. Complementary methods have been developed to damp the wakes, which are created by each bunch, before the next bunch arrives :

- the detuning technique introduces a spread in deflecting mode frequencies, resulting in decoherence of the excited fields.

- the damping technique uses special devices, which extract the induced higher order modes power.

Experiments with beam at SLAC with the so called 'Damped Detuned Structures', where the frequency spread is obtained by a variation of the iris dimension and pumping slots are used for damping of the modes[9], gave very good agreement with theoretical predictions. A sketch of this 'DDS' structure, as well as the dipole wake function (theoretical curve and experimental points) as a function of the distance (in meters) behind the driving bunch are shown on Fig.6. The transverse strength has been reduced by a factor 100, in such a way
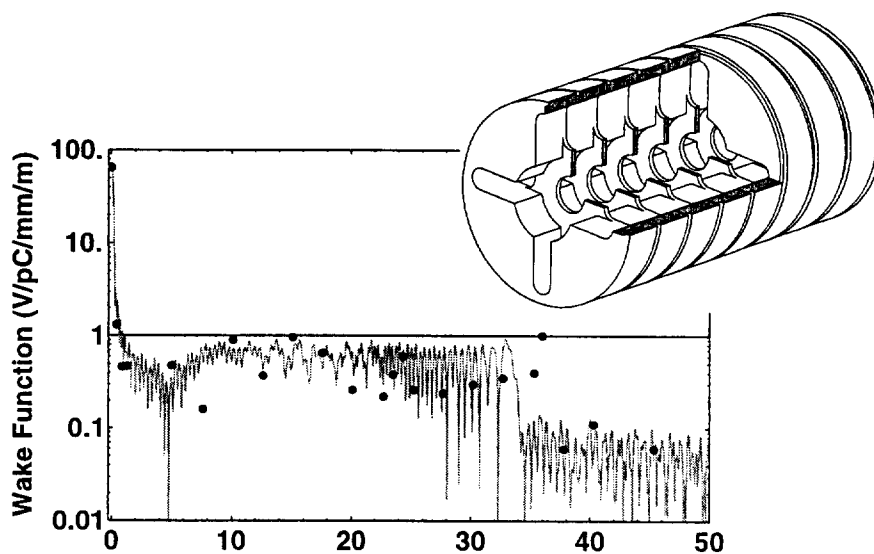

Figure 6: Transverse wake function of the NLC Damped Detuned Structure.

that the wakefield is damped below the limit required by the NLC design. In addition, the damping manifolds provide a straightforward method of measuring the misalignment of the structure by monitoring of the induced dipole modes.

Dispersive and chromatic effects

Another harmful effect on the beam emittance is the dispersive or chromatic effect. When the beam passes off-center through a focusing magnet, the particles of a bunch with a finite energy spread receive different deflections. Fig.7 shows, for example, the results of a simulation on a linac with misaligned quadrupoles and beam position monitors (only a few magnets are drawn). The wandering curve represents the final beam orbit after steering to the quadrupole center. The transverse phase space (bottom) gives the information about the emittance growth of about 200 % for this case. Assuming that the quadrupole are randomly

8

misaligned and that the beam is steered to the center of the quadrupoles, the analytical expression of the final emittance growth Eq.6 states that the designs with relatively large energy spread and strong focusing will demand more severe tolerances.

$$\frac{\Delta \varepsilon}{\varepsilon} \propto \frac{\delta_c^2 F(foc)}{\varepsilon} \frac{\gamma_o^2}{G} d_{rms}^2 \tag{6}$$

with the initial Lorentz factor γ_o, the rms correlated energy spread δ_c, the gradient G, the total BPM alignment error relative to the centerline d_{rms} and the function $F(foc)$ describing the focusing strength.

The order of magnitude of the tolerances (μm) on the quadrupole and BPM (assumed attached to the quadrupole) positionning for the different designs is summarized in Table 3.

Table 3: tolerances (μm) on the quad and BPM positionning

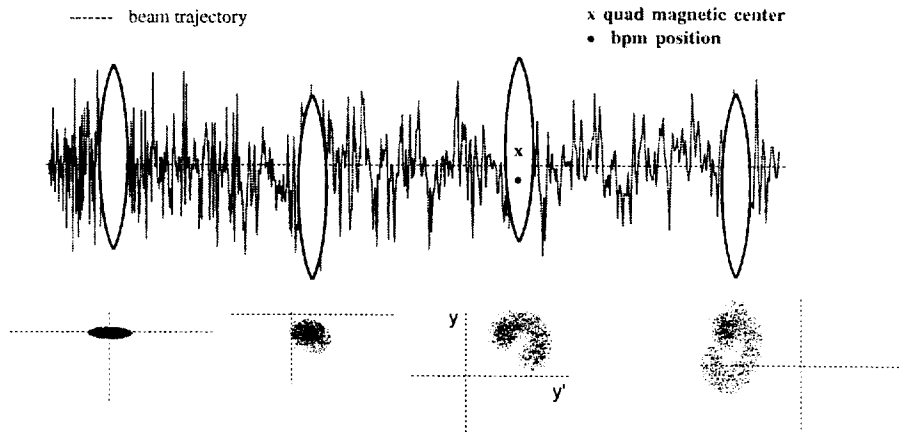| TESLA	SBLC	JLC	NLC	CLIC
100	2	1	3	0.5

Figure 7: Beam trajectory due to quadrupole and BPM misalignments.

2.4 Ground motion

Ground motion is of major concern in future linear colliders because it will displace focusing magnets, which, in turn, will dilute the beam emittance in the linac, induce transverse offsets of the opposite beams and spot sizes at the interaction point. Much data exist now on ground motion and the power spectra exhibit about the same behaviour at different locations. They grow very fast with decreasing frequency, behaving as ω^{-4} on a wide frequency band with a noticeable peak around 0.1 Hz, due to ocean waves. Cultural noise generally dominates over the natural noise for frequencies above 1 Hz. Future colliders must be properly designed to reduce the vibration level caused by pumping devices, water flow ..., as much as possible.

9

From correlation measurements (at CERN, SLAC) with two separated seismometers, the ground motion could be well modeled.

At very low frequency, the motion is purely random and quite large. This diffusive motion is usually described by the 'ATL' law, which states that the variance of relative displacements grow linearly with time and separation between two points:

$$\Delta y_{rms}^2 = A \cdot T \cdot L \qquad \text{with} \quad A = 10^{-7} \text{to} 10^{-5} \mu\text{m}^2/\text{s}/\text{m}$$

with the parameter A depending on the location.

At higher frequency, the motion is predominantly wave-like and is well described by transverse plane waves, propagating with isotropic distribution in direction. Fortunately, for long spatial periods, the effects will be suppressed by the lattice response and should not impact the luminosity. However, orbit feedbacks should correct the effects induced by short spatial periods, less than the betatron beam oscillation length, and by the small random component of the motion. But small emittances with strong focussing in the linac and small spot sizes in the final focus will require high feedback performances, in terms of correction periodicity, BPM resolution, electronics drifts ...

Fig.8 gives the emittance growth as a function of time for diffusive ground motion. Assuming a parameter $A = 10^{-5} \mu\text{m}^2/\text{s}/\text{m}$, a simple re-steering every 1 or 2 hours is sufficient for limiting the dilution below 20%, while a new beam-based alignment is necessary every 5 years, when the dilution is too large, even with feedback loops.
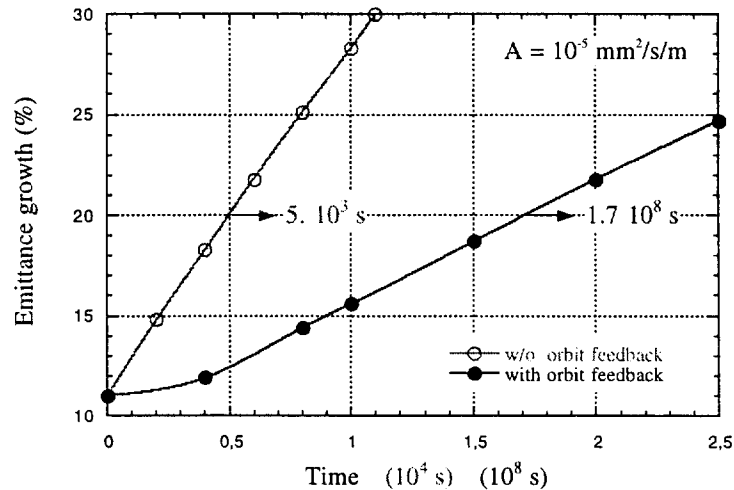

Figure 8: Emittance growth without (empty circles) and with (black circles) orbit feedback due to diffusive ground motion in TESLA linac.

2.5 Interaction region and diagnostics

The interaction region consists mainly of the final focus system, which provides the beam size demagnification with the proper correction of the chromatic aberrations, and the collimation system, which provides a protection from background caused by large amplitude

10

particles. Furthermore, a 'Big Bend', between collimation and final focus can help to reduce background due to muons originating from the collimators. Lastly, the disrupted beams and the beamstrahlung must be removed from the interaction region.

The separation between the outgoing beam and the incoming beam is generally provided by a crossing angle, to avoid parasitic interactions between the bunch trains travelling in opposite directions. While a large angle can ease the exit of the disrupted beams, which must pass freely through the final quadrupole aperture, it needs however a 'crab-crossing' system to make the bunches colinear during the collision in order to maintain the full luminosity potential.

In the TESLA design, since first parasitic interaction occurs at large distance from the IP, head-on collision can be used. The beams are separated after the final quadrupole doublet by electrostic deflectors. In this scheme, superconducting quadrupoles provide a large aperture for the disrupted beams and beamstrahlung photons, and synchrotron radiation generated in the final doublet on the opposite side. Fig.9 shows for example the envelopes of the synchrotron radiation emitted in the last quadrupoles through the vertex detector and opposing doublet apertures, in the vertical plane. Because of the very small
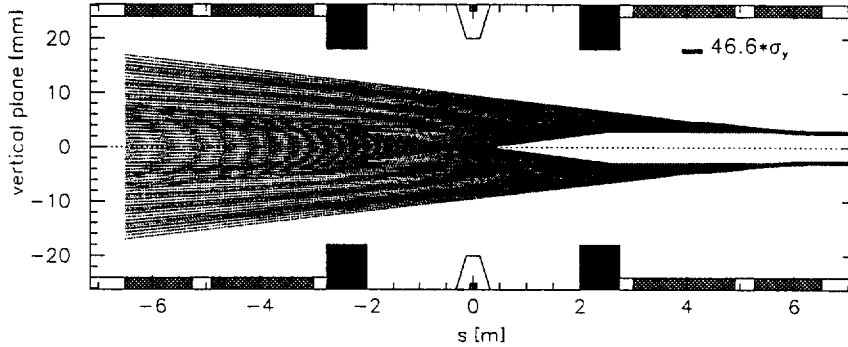

Figure 9: Synchrotron radiation emitted in the last TESLA doublet (vertical plane).

beam sizes, beam diagnostics at the interaction point is a critical issue, in particular for the collider tuning. First, beam-beam deflection scans are very useful to steer and to maintain the beam into collision. Due to the disruption, the bunches are more or less deflected during the collision, according to their relative displacement. Such a scan, performed at SLC during a 94' run with flat beams is reproduced on Fig.10. The beam size can even be inferred from a fit to the deflection, unless the disruption is so large that the slope of the deflection angle is nearly insensitive to the beam offset. Other tools can then be used, like the detection of low-angle radiative Bhabha pairs e^+e^- after the IP, within an energy range discriminating the disrupted beam due to beamstrahlung effects and the particles due to pair production.

A direct measurement of the beam sizes requires sub-micron diagnostics. The laser wire scanner uses an intense laser focused to narrow spot; the beam size is inferred from the rate of Compton backscattering when the beam is scanned across the laser spot. Beam sizes down to 1 μm have been measured at the SLC detector but are still to large with respect to the
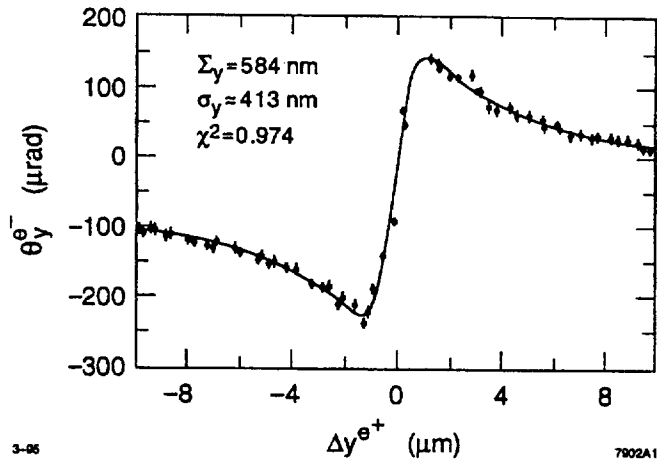
Figure 10: Beam-beam deflection scan at SLC (vertical plane).

envisaged beam dimensions. The laser interferometer ('Shintake-Monitor') uses Compton scattering of photons in a laser interference pattern; the beam sizes corresponds to the depth of the photon rate modulation, when the beam is scanned across the fringe pattern (Fig.11). Beam sizes as small as 70 nm have been measured at the Final Focus Test Beam (FFTB) at SLAC. The minimal spot size is limited by the available lasers and is around 10 nm.
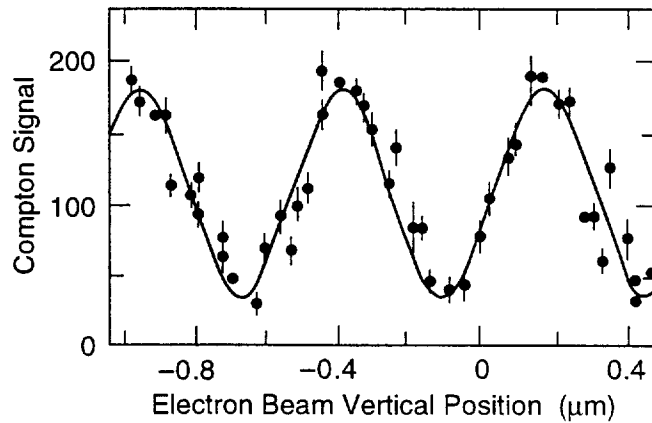

Figure 11: Beam size measurement at FFTB with a laser interferometer (modulation of the photon rate when the beam is scanned across the 0.5 μm long fringe pattern.

3   Test Facilities for Linear Colliders

Several test facilities around the world seek to test the critical issues of the various approaches, putting the emphasis on 3 primary areas.

12

- Creating the low emittance beams in injectors and damping rings : the Accelerator Test Facility at KEK

- Accelerating the beams in the high energy linac : the TESLA Test Facity at DESY, the S-Band Test Facity at DESY, the NLC Test Accelerator at SLAC, the CLIC Test facility at CERN

- Focusing the beams to a small spot in the final focus : the Final Focus Test Beam at SLAC, where very small vertical beam size as low as 70 nm have been measured.

In addition, we should mention the development of efficient high peak power RF sources at SLAC and BINP and the study of the drive beam generation for the Two-Beam sceme, at CESTA (near Bordeaux), where the self-bunching properties of a Free Electron Laser are used to bunch a high intensity beam coming from an induction linac, and at LLBL (Berkeley), where the principle of the relativistic klystron will be tested. Last, the SLC allows the testing of new ideas or new components with high energy electron beams.

The Accelerator Test Facility consists of 3 major parts : an S-Band injector, a damping ring and a bunch compressor, with the aim of achieving a vertical emittance of the order of 5×10^{-8} rad.m and 100 μm long bunches. For this purpose, a strong focusing lattice with a fine magnet alignment system was especially designed, a new damped RF cavity to suppress the coupled bunch instabilities was developed and sophisticated beam diagnostics, including beam size monitors using synchrotron radiation were installed. The first beam commissionning at a lower energy (around 1 GeV) occured in January-April 1997. The next efforts will focus on the low vertical emittance and damping time in the ring.

The S-Band Test Facility attempts to push to its limit the present standard technology at low frequency. The test linac of 450 MeV final energy consists of an injector providing a bunch train similar to the one considered for the full scale collider and four 6 meter long accelerator structures, powered by two 150 MW klystrons of 3 μs pulse length. The two klystrons, which are based on the existing technology, were built at SLAC and have been successfully tested. The accelerating sections will be aligned by means of micromovers, one on each end of the girder. Special attention must be paid to achieve the final tight straightness required from the tolerable transverse mode excitation. Anti-vibrational quadrupole have been developed to alleviate the effects of ground motion. They are supported by stiff concrete, pushing away mechanical resonances well beyond 100 Hz, and are equipped with accelerometers to feed back on vertical motion via piezo movers.

The NLC Test Accelerator [11] is a high gradient X-Band linac, which consists of an injector, with the same average current as required in the NLC design, a chicane for magnetic bunch compression, six accelerator sections of length 1.8 meter, and a spectrometer for bunch train analysis after acceleration. The sections are powered in pairs by 50 MW klystrons, whose peak power is nearly quadrupled by RF pulse compression, reaching a field gradient of 50 MV/m and loaded to 37 MV/m by the nominal beam current. A future upgrade, similar to the NLC upgrade from 0.5 to 1 TeV, is planned by installing 75 MW klystrons and doubling their number. Fig.12 shows the power measurement of the RF pulse compression system. The 50 MW power, coming from the klystron, resonantly charges two delay lines. After several round trip times, the klystron phase is suddenly flipped by 180
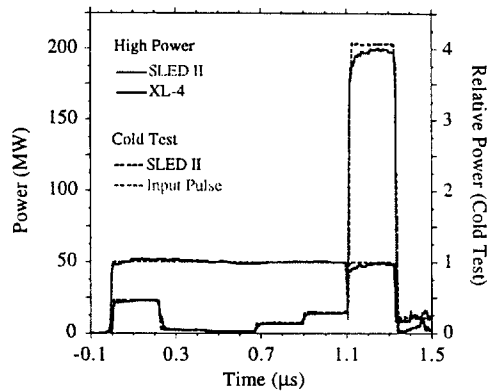
Figure 12: Power test of pulse compression system

deg, creating a large compressed pulse of 200 MW RF power. Another crucial issue for the multibunch beam is the beam loading compensation. Without compensation, the energy drop would be 20 to 30 % between the head and the tail of the multibunch train. By shaping of the RF pulse during the filling of the accelerating structure, the energy spread could be reduced down to the 10^{-3} level.

The CLIC Test facility [13], operating at 30 GHz, makes use of the highest frequency structures. High power tests up to 120 MV/m have showed that high accelerating fields could be achieved, with negligible dark current and without long RF conditionning. Generation of a high intensity drive beam with short bunches by means of a laser-driven RF gun, production of 75 MW of RF power by decelerating a train of 24 bunches (corresponding to a field of 125 MV/m) and acceleration of this probe beam by the power so generated (with a field gradient of 90 MV/m) were the main results obtained during the first phase of the facility. The goal of the second phase, under installation, is to demonstrate, at a larger scale, the feasibility of the Two Beam Accelerator scheme. A peak RF power of 480 MW will be produced at 30 GHz from the drive beam and the probe beam will be accelerated up to 320 MeV. A sketch of the facility is shown on Fig.13. It will include a string of six transfer structures, each of them feeding two accelerating sections with 40 MW RF power. The drive beam is accelerated by means of two travelling wave structures, running at two slightly different frequencies, to compensate for the very high beam loading.

VLEPP developments : At Novosibirsk, the efforts concentrate on RF peak power sources. A gridded klystron was developed at 14 GHz, with high efficiency. It uses a periodic permanent magnet focusing to save the extra power that is consumed by conventional technology. A peak RF power of 60 MW was achieved.

The TESLA Test Facity [12] at DESY is under construction at DESY by an international collaboration. The main objectives are

- to accelerate a beam with proper qualities through a chain of 24 superconducting cavities, operating at a gradient of at least 15 MV/m.

- to reach an overall design of cavities, cryostats, couplers and auxiliary systems, at a cost being competitive with room temperature designs.
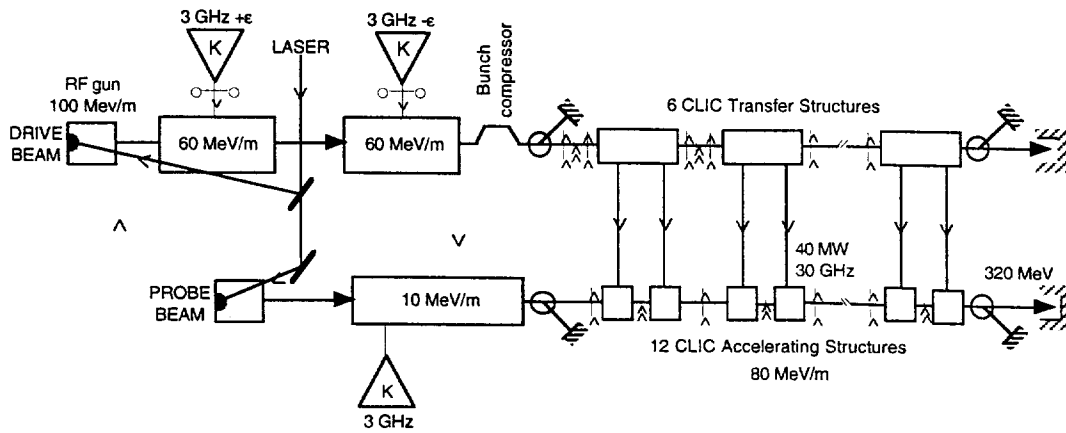
14

Figure 13: Sketch of the CLIC Test Facility, Phase II.

An infrastructure to process and to test the cavities includes a complex of clean rooms and a chemical etching installation for cavity treatment and assembly, vertical and horizontal cryostats for cavity testing and an area for the assembly of the whole cryomodule. The 380 MeV TTF linac consists of a first injector, with a beam current similar to the collider design, but at lower charge per bunch, and a first 8 cavity module. The second and third cryomodules, as well as a second injector, based on a laser-driven RF gun, will be ready in 1998. Lastly, bunch compressors and an undulator will be installed in 1999 for testing a Free Electron Laser, operating in the 'Self Amplified Spontaneous Emission' mode. A first electron beam was accelerated through the first cryomodule and transported to the final spectrometer. The average accelerating gradient was 16.7 MV/m, bringing the beam energy to 125 MeV. The best TTF cavities, which were previously tested in vertical cyostat, have gradients exceeding 20 MV/m with quality factors Q_0 around 5×10^9. Their excitation curves are plotted on Fig.14. However, a number of cavities have revealed some limitations which are now understood. For one company, for example, there were systematic premature breakdowns and were identified as bad weldings at the equator of the cells. Lastly, material defects can greatly affect the gradient performance. Using high quality niobium sheets will improve the situation. In the future, it is planned to eliminate the defective sheets after eddy-current scanning. In addition to reliable high gradient and high Q operation, specific issues will be addressed in the near future, like the heat leak of the cryostat, the alignment stability of the cavities and quadrupoles, the pulsed RF operation, the higher order mode losses, as well as wakefields measurements.

4   Muon Colliders

The possibility of muon colliders was introduced in the early 70', by Krinsky, Neuffer and others [14,15]. The attractive scheme comes mainly from the larger mass of muon with respect to electrons. They produce much less synchrotron radiation and s-channel studies of Higgs production is possible. The consequent advantages are the following:
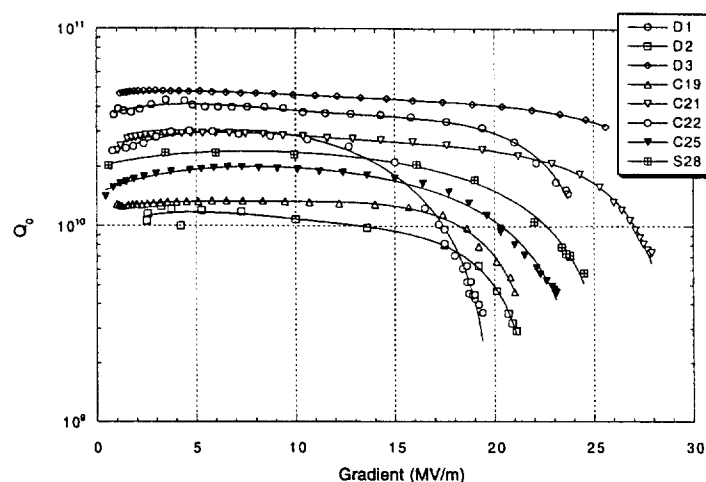
15

Figure 14: Excitation curves Q(Eacc) of the best TTF cavities.

- Like electrons, the full energy is available for new particles production

- Like protons, they can be accelerated at high energies and stored in circular rings with high-field bending magnets, much smaller than the linacs needed for electrons; high luminosity can hence be obtained through the use of the same particles for more than 1000 bunch crossings

- Last but not least, beamstrahlung is much reduced, resulting in a smaller energy loss and a narrow energy spread; besides, the ratio beam power over vertical spot size can be much looser

The critical property, however, is the decays of muons into electrons and neutrinos (with a lifetime of 2.2 μs at rest and about 40 ms at 2 TeV). The electrons will induce, by synchrotron radiation, a heat load on the superconducting magnets of the collider ring, which will need to be protected by a tungsten liner. On the other hand, the muon decay will cause a large background in the detector, comparable to the one produced at the LHC interaction point. In addition to an efficient collimation system located far from the collision point, the detector must be shielded by a tungsten cone, extended down towards the vertex. Surprisingly, the flux of decay neutrinos can also, at high energy, become a significant radiation hazard [17]. In fact, the very small neutrino cross-section is compensated by the huge number of high energy neutrinos (of the order of 10^{21} per year) and the tight collimation of the neutrino beam. The radiation dose, with a cubic dependence on energy, appears low enough for lower energy muon colliders, but could reach unacceptable levels for multi-TeV colliders, which will need to be located sufficiently deep underground.

16

4.1 The basic components

In order to reach high energy muons with high intensity and relatively good quality, the particles must travel through a cascade of components (see Fig.15. A proton source produces
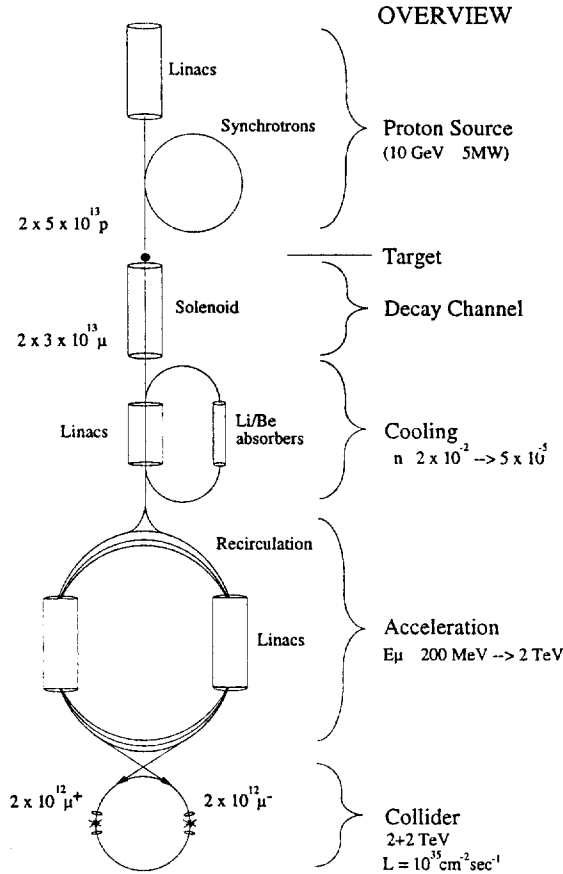

Figure 15: Schematic drawing of basic components of a muon collider.

a high intensity proton beam, which is focussed on a heavy metal target. The pions generated are captured by a high field solenoid and transferred to a solenoidal decay channel, where the momentum spread of the pions and muons is reduecd by phase rotation through low-frequency linacs. The diffuse muons bunches from the decay channel are then cooled by a sequence of 20 to 30 ionization cooling stages to shrink their emittances by more than two order of magnitude. Because of the short muon lifetime, they must be rapidly accelerated in recirculating linacs or fast pulsed synchrotrons. Last, the $\mu^+\mu^-$ bunches can collide in a storage ring, where they only survive for about 1000 turns and must be hence frequently refreshed. Even though first studies concentrated on multi-TeV colliders, design scenarios at lower energies, especially on an s-channel Higgs factory operating at around $100\,\text{GeV}$, are now carried out in parallel. Table 4 gives possible parameters of the 4 TeV collider and

17

a 100 GeV 'Higgs Factory', for which two modes of operation are envisaged: with maximum luminosity or with minimum momentum spread for precision measurements [17].

Table 4: Parameters of a 4 TeV and 100 GeV c.m. energy machines

c.m. Energy	GeV	4000	100	
p Energy	GeV	16	16	
p's/bunch	10^{13}	2.5	5	
rep x $n_{bunches}$	Hz	30	15	
p power	MW	4	4	
muons/bunch	10^{12}	2	4	
collider circ	m	8000	260	
ℓ^* at IP	m	6.5	5	
4 x σ_θ at IP	mrad	3.5	8	
dp/p	%	.12	.12	.003
rms ϵ_n	π mm mrad	50	85	280
β^*	cm	0.3	4	13
σ_z	cm	0.3	4	13
σ_r	μm	2.8	82	270
tune shift		0.04	0.05	0.015
luminosity	$cm^{-2}sec^{-1}$	10^{35}	1.2×10^{32}	10^{31}

4.2   The ionization cooling

Once the large number of muons have been collected, their emittances must be fairly shrinked - by 3 orders and 1 order of magnitude in the transverse and longitudinal planes, respectively - within the muon lifetime to achieve the luminosity. Fig.16 illustrates schematically the basic principle: the beam passes through a material medium, like lithium or beryllium, and loses both transverse and longitudinal momemta; after coherent re-acceleration, the longitudinal momentum is restored, leaving a net loss of transverse momentum. Unlike protons and electrons, this type of cooling is well suited to muons, because of their relatively low nuclear cross section and bremstrahlung. However, the process exhibits a limit, when the heating, due to multiple scattering is balanced by the cooling due to energy loss. The heating is minimized by using strong focusing and low-Z absorber. Concerning the energy spread reduction, one has to resort to an indirect method: dispersion and Be or Li wedges introduce some transverse variation in absorber density, where the position is energy dependent. Finally, the longitudinal emittance is reduced, but at the expense of increase of the transverse emittance. The cooling system will thus include a series of cooling stages, each of them consisting of low beta sections (FOFO lattices with alternating solenoids at the early stages and current lithium rods at the later stages), dispersive sections (to interchange longitudinal and transverse emittances) and a linac to restore the energy lost in the absorbers.
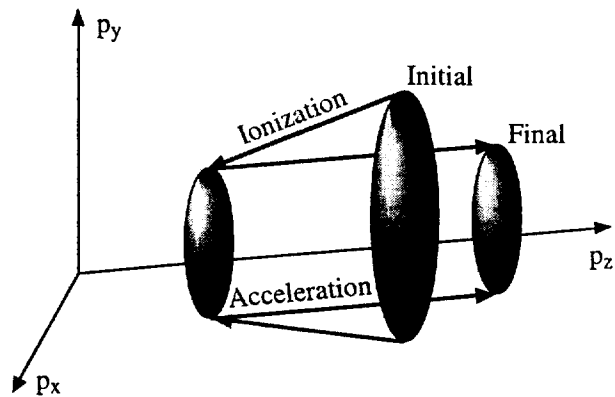
18

Figure 16: Schematic view of ionization cooling in momentum space.

4.3   R and D program for muon collider

Lot of progress has been made on the theoritical studies, but the feasibility of such a collider requires significant experimental programs. A short term R and D might focus on the most critical parts - ionization cooling and the production and capture of large pion bunches - and include the construction of dedicated important experimental facilities. A long term R and D effort, on a ten years time scale, would consist of a more extensive experimental program, prior to construction of a first muon collider. The objectives would be to achieve the muon production and to demonstrate the cooling process with the actual required high intensity bunches.

5   Conclusion

A next e^+e^- linear collider is a clean way to complement the LHC and can be realized very soon. Present designs, in the 0.5-1 TeV c.m. energy range, have come to maturity and are the results of extensive research and collaborative effort of scientists from many laboratories, over the last ten years.

Extension to energies above 2 TeV will be certainly difficult for achieving the desired luminosities with reasonable beamstrahlung. In any case, the only way is to decrease the vertical emittance, which has however a lower limit coming, in particular, from damping ring and emittance preservation during transport through the main linac.

A muon collider could be a future alternative to go to higher energies. The challenges are, however, many and a lot of Research and Development on the cooling principle and investigations on the neutrino radiation hazard, for example, are needed to demonstrate its feasibility.

19

Acknowledgments

References

1. *JLC-I*, KEK Report 92-16, (1992).
2. *Zeroth-Order Design Report for the Next Linear Collider*, SLAC Report 474 (1996).
3. *Conceptual Design of a 500 GeV e^+e^- Linear Collider With Integrated X-ray Laser Facility*, DESY Report 1997-048 (1997).
4. J.P. Delahaye, *Design Issues of TeV Linear Colliders*, Proc. of the 5th European Part. Acc. Conf., Sitges (1996).
5. R. Brinkmann *Status of the Design for the TESLA Linear Collider*, Proc. of the Part. Acc. Conf., Dallas (1995).
6. P. Chen, *An introduction to Beamstahlung and Disruption*, Frontiers of Particle Beams **296**, Springer-Verlag (1986).
7. R.H. Siemann, 7th Workshop on Advanced Accelerator Concepts, Lake Tahoe CA, SLAC-PUB-7394 (1997)
8. R.W. Assmann, *Beam Dynamics in SLC*, Proc. of the Part. Acc. Conf., Vancouver (1997), to be published.
9. N.M. Kroll, *The SLAC Damped Detuned Structure: Concept and Design*, Proc. of the Part. Acc. Conf., Vancouver (1997), to be published.
10. T.O. Raubenheimer, Proc. of Linac Conf., CERN (1996).
11. R.D. Ruth *et al*, *Results from the SLAC NLC Test Accelerator*, SLAC-PUB-7532, Proc. of the Part. Acc. Conf., Vancouver (1997), to be published.
12. B. Aune *et al*, *Results from the TESLA Test Facility at DESY*, Proc. of the Part. Acc. Conf., Vancouver (1997), to be published.
13. H.H. Braun *et al*, *Results from the CLIC Test Facility*, Proc. of the 5th European Part. Acc. Conf., Sitges (1996).
14. A.N. Skrinsky and V.V. Parkhomchuk, Sov. J. of Nucl. Physics **12**, (1981) 3.
15. D. Neuffer, IEEE Trans. **NS-28**, (1981) 2034.
16. R.B. Palmer *et al*, *Muon Colliders*, Proc. of the 9th ICFA Workshop on Advanced Beam Dynamics and Technology Issues for $\mu^+\mu^-$ Colliders, Montauk, New York (1995).
17. R.B. Palmer, *Progress on $\mu^+\mu^-$ Colliders*, Proc. of the Part. Acc. Conf., Vancouver (1997), to be published.
18. N.V. Mokhov, *Comparison of Backgrounds in Detectors for LHC, NLC and $\mu^+\mu^-$ Colliders*, Proc. of the Symposium on Physics Potential and Development of $\mu^+\mu^-$ Colliders, San Francisco (1995).
19. D. Neuffer, *Beam Dynamics problems for a $\mu^+\mu^-$ Collider*, Proc. of the Part. Acc. Conf., Vancouver (1997), to be published.